

## Thermoelastic Properties of Cadmium Fluoride†

S. ALTEROVITZ AND D. GERLICH\*

*Department of Physics and Astronomy, Tel Aviv University, Ramat Aviv, Israel*

(Received 5 November 1969)

The second-order elastic moduli, as well as their temperature and pressure derivatives, and the thermal expansion of single-crystal  $\text{CdF}_2$  were determined at room temperature. The values of the elastic moduli (in units of  $10^{11}$  dyn/cm<sup>2</sup>) are  $c_{11}=18.270$ ,  $c_{12}=6.674$ , and  $c_{44}=2.175$ . The measured values of the temperature derivatives (in units of  $10^{-4}$  deg<sup>-1</sup>) are  $d \ln c_{11}/dT = -3.71$ ,  $d \ln c_{12}/dT = -5.08$ , and  $d \ln c_{44}/dT = -5.33$ ; the pressure derivatives are  $dc_{11}/dP = 7.11$ ,  $dc_{12}/dP = 5.52$ , and  $dc_{44}/dP = 1.35$ ; the thermal expansion is  $2.2 \times 10^{-5}$  deg<sup>-1</sup>. From the elastic data, a Debye temperature of 328°K was deduced. The experimentally measured values of  $c_{44}$  and the pressure derivatives were compared with theoretically calculated ones. Good agreement was found for the pressure derivatives, while a large discrepancy for  $c_{44}$  was noted. The possible reasons for these correlations and the conclusions pertaining to the lattice interactions in  $\text{CdF}_2$  are discussed.

### I. INTRODUCTION

THE thermoelastic properties of  $\text{CdF}_2$  are of interest on several counts. Very few data about the lattice properties of the material are available. Also,  $\text{CdF}_2$  is closely related to  $\text{CaF}_2$ , both having the same structure, the same anion, and nearly the same unit-cell size (5.388 Å versus 5.453 Å). In addition, the ionic radii for the cations are nearly the same. Thus, any differences between the elastic properties of  $\text{CaF}_2$  and  $\text{CdF}_2$  should be mainly dependent on the difference in the inner electronic structures of  $\text{Cd}^{++}$  and  $\text{Ca}^{++}$ , as the elastic properties are independent of the nuclear mass.<sup>1,2</sup> The elastic properties of  $\text{CaF}_2$  have been extensively investigated<sup>3-7</sup>; thus it may be possible to deduce the effect of the electronic structure on the elastic properties by studying the latter in  $\text{CdF}_2$ . With this in mind, a study of the thermoelastic properties of single-crystal  $\text{CdF}_2$  was undertaken. The room-temperature second-order elastic moduli (SOEM), as well as their temperature and pressure derivatives, were measured. The experimentally determined quantities were compared with theoretically calculated ones, and some conclusions pertaining to the lattice forces in  $\text{CdF}_2$  are drawn.

### II. EXPERIMENTAL

The sample used in the present study was cut from a single-crystal boule of  $\text{CdF}_2$ , grown by the Koch-Light Laboratories. The boule was oriented, and a right

parallelepiped with faces corresponding to (110), ( $\bar{1}10$ ) and (001) crystalline planes cut, by the RCA Laboratories. The cut sample was handlapped until opposite faces were parallel to within a few parts in  $10^5$ , and then the orientation was checked by x-ray Laue backreflection. The faces were found to correspond to the crystalline planes to within  $\frac{1}{2}^\circ$ . The final size of the sample was  $11 \times 19 \times 19$  mm.

Cadmium fluoride, being cubic, has three independent SOEM:  $c_{11}$ ,  $c_{12}$ , and  $c_{44}$ . The latter were determined from the absolute value of the sound velocity, while from the changes in this velocity with hydrostatic pressure and with temperature, the derivatives were determined. With the available sample, five different sound propagation modes could be utilized, and the three SOEM and their derivatives were computed by a least-squares fit.

The sound waves were generated by means of X- and Y-cut crystalline quartz transducers, operating at their fundamental frequency of 15 MHz. The transducers were bonded to the samples with phenylsalicylate (salol).

The absolute value of the sound velocity was measured by the McSkimin pulse-superposition method,<sup>8,9</sup> while the changes in the sound velocity with temperature and pressure were determined by the frequency-modulated pulse-superposition method.<sup>10,11</sup> The temperature of the sample was monitored carefully at all times, and all the results with the changes in pressure were normalized to 295°K.

The absolute value of the sound velocity was determined in a manner described previously.<sup>12</sup> The accuracy in each single measurement was one part in  $10^4$ ; however, the over-all error in the SOEM is larger, owing to possible deviation of the directions of the sound propagation from the crystalline axis, and to errors in the

† Based on a thesis submitted by S. Alterovitz to the Tel Aviv University in partial fulfillment of the requirements for a Ph.D. degree.

\* On sabbatical leave at ARX, Aerospace Research Laboratories, Wright-Patterson Air Force Base, Dayton, Ohio 45433.

<sup>1</sup> M. Born and K. Huang, *Dynamical Theory of Crystal Lattices* (Oxford U. P., New York, 1954).

<sup>2</sup> R. A. Cowley, Proc. Roy. Soc. (London) **A268**, 121 (1962).

<sup>3</sup> D. R. Huffman and M. H. Norwood, Phys. Rev. **117**, 709 (1960).

<sup>4</sup> C. Wong and D. E. Schuele, J. Phys. Chem. Solids **28**, 1225 (1967).

<sup>5</sup> C. Wong and D. E. Schuele, J. Phys. Chem. Solids **29**, 1309 (1968).

<sup>6</sup> P. S. Ho and A. L. Ruoff, Phys. Rev. **161**, 864 (1967).

<sup>7</sup> S. Alterovitz and D. Gerlich, Phys. Rev. **184**, 999 (1969).

<sup>8</sup> H. J. McSkimin, J. Acoust. Soc. Am. **33**, 12 (1961).

<sup>9</sup> H. J. McSkimin and P. Andreatch, Jr., J. Acoust. Soc. Am. **34**, 609 (1962).

<sup>10</sup> H. J. McSkimin, J. Acoust. Soc. Am. **37**, 864 (1965).

<sup>11</sup> H. J. McSkimin and P. Andreatch, Jr., J. Acoust. Soc. Am. **41**, 1052 (1967).

<sup>12</sup> S. Alterovitz and D. Gerlich Phys. Rev. B **1**, 2718 (1970).

TABLE I. Sound transit times for the different modes of propagation.

Mode No.	Propagation direction	Polarization direction	Length (cm)	Transit time ( $\mu$ sec)	$\rho v^2$ ( $10^{11}$ dyn/cm $^2$ )
1	[110]	[001]	1.1279 $\pm$ 0.00005	12.2474 $\pm$ 0.0015	2.1740 $\pm$ 0.0005
2	[110]	[110]	1.1297 $\pm$ 0.00005	4.716 $\pm$ 0.002	14.657 $\pm$ 0.014
3	[110]	[110]	1.1297 $\pm$ 0.00005	7.4966 $\pm$ 0.0007	5.8006 $\pm$ 0.0015
4	[001]	[001]	1.9230 $\pm$ 0.00005	7.1907 $\pm$ 0.0005	18.268 $\pm$ 0.0035
5	[001]	(001) plane	1.9230 $\pm$ 0.00005	20.8442 $\pm$ 0.0018	2.1733 $\pm$ 0.0007

TABLE II. SOEM of CdF $_2$  at 295 $^\circ$ K. (Units are  $10^{11}$  dyn/cm $^2$ .)

$c_{11}$	$c_{12}$	$c_{44}$	$B^S$	$B^T$
18.270 $\pm$ 0.0026	6.6744 $\pm$ 0.0059	2.175 $\pm$ 0.0022	10.5396 $\pm$ 0.0048	10.06 $\pm$ 0.12

temperature normalization, polarization direction, and transducer resonant frequency. The thermal expansion was measured directly, using a Johansson Mikrokator dial gauge. The sample was sandwiched between two fused silica blocks, and heated with a stream of hot air. The setup was calibrated with crystals of CaF $_2$  and SrF $_2$ , and agreement within 10% of another independent measurement<sup>13</sup> was found.

### III. RESULTS

The linear thermal expansion at room temperature was determined as  $(22\pm 2)\times 10^{-6}$  deg $^{-1}$ . The room-temperature density was measured by the weight-displacement method and found to be  $6.386\pm 0.002$  g/cm $^3$ , which agrees very well with the x-ray value.<sup>14</sup>

Table I shows the values of the round trip travel time  $t$  for the five different modes of sound propagation. From the latter data, the three SOEM were calculated by a least-squares fit, and are shown in Table II. From the values of the SOEM, the magnitude of  $\rho v^2$  in any direction may be calculated; here,  $\rho$  is the density and  $v$  is the sound velocity. The values of  $\rho v^2$  for some directions of high symmetry are shown in Fig. 1. Here 3 refers to the longitudinal mode; 1 and 2 refer to the slow and fast shear modes, respectively. It is evident from Fig. 1 that CdF $_2$  is elastically highly anisotropic.

The changes in the sound velocity with temperature and pressure are summarized in Tables III and IV and Figs. 2-5. The dots in the figures represent the measured reciprocal resonant frequency for all of the five possible modes of propagation as a function of the temperature and applied hydrostatic pressure.

The straight lines are least-squares fits to the experimental data. As can be seen from the graphs, the changes in the sound velocity are linear over the whole of the measured range, within experimental error.

From the slopes of the lines in Figs. 2-5, the tem-

perature and pressure derivatives were determined from the following equations:

$$\frac{d \ln c_{ij}}{dT} = -\alpha - 2 \frac{d \ln t}{dT}, \quad (1)$$

$$\frac{dc_{ij}}{dP} = \frac{c_{ij}}{3B^T} + \left( \frac{d(\rho_0 W^2)}{dP} \right)_{P=0}. \quad (2)$$

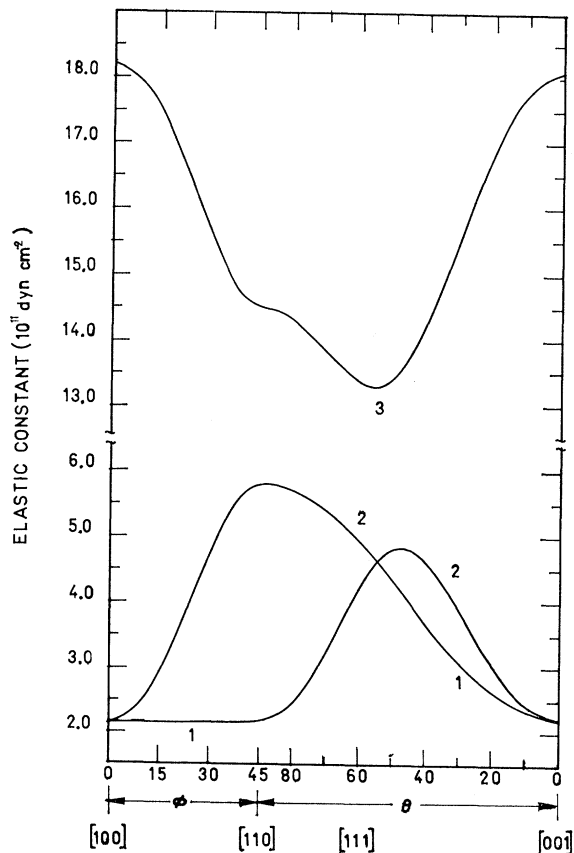


Fig. 1. Values of  $\rho v^2$  for some directions of high symmetry.

<sup>13</sup> A. C. Bailey and B. Yates, Proc. Phys. Soc. (London) 91, 390 (1967).

<sup>14</sup> J. D. H. Donnay, A. C. A. Monograph 5 (Geological Society, New York, 1964).

TABLE III. Temperature dependence of the sound travel time for the five propagation modes.

Mode No.	Propagation direction	Polarization direction	$\rho v^2$	$\frac{d \ln t}{dT} \times (10^{-6} \text{ deg}^{-1})$	$\left(\frac{d \ln c}{dT}\right)_P \times (10^{-4} \text{ deg}^{-1})$
1	[110]	[001]	$c_{44}$	$255.4 \pm 0.2$	$-5.328 \pm 0.024$
2	[110]	[110]	$\frac{1}{2}(c_{11} + c_{12} + 2c_{44})$	$202.8 \pm 0.6$	$-4.276 \pm 0.033$
3	[110]	[110]	$\frac{1}{2}(c_{11} - c_{12})$	$137.8 \pm 0.4$	$-2.976 \pm 0.028$
4	[001]	[001]	$c_{11}$	$174.1 \pm 0.1$	$-3.702 \pm 0.013$
5	[001]	(001) plane	$c_{44}$	$252.3 \pm 0.4$	$-5.266 \pm 0.027$

Here,  $c_{ij}$  is the effective elastic modulus, viz.,  $\rho v^2$ ,  $\alpha$  is the linear thermal expansion,  $B^T$  is the isothermal bulk modulus,  $\rho_0$  is the zero-pressure density, and  $W$  is the "natural" velocity<sup>15</sup> ( $W = L_0/t$ , where  $L_0$  is the zero-pressure length of the sound path).  $B^T$  was deduced from the following equations:

$$B^T = B^S(C_V/C_p), \quad (3)$$

$$C_p - C_V = (3\alpha)^2 B^S T V / C_p, \quad (4)$$

where  $C_p$  and  $C_V$  are the specific heat at constant pressure and volume,  $V$  is the volume,  $B^S$  is the adiabatic bulk modulus, and  $T$  is the absolute temperature.

As specific-heat data for  $\text{CdF}_2$  are not available, the Debye model was utilized in calculating the specific

heat of  $\text{CdF}_2$ . The Debye temperature was computed from the elastic data as described hereafter, and from it the room-temperature value of  $C_V$  for  $\text{CdF}_2$  was determined as 70 J/mole deg.

The validity of the procedure was checked by computing in the same manner the room-temperature specific heats of  $\text{CaF}_2$ ,  $\text{SrF}_2$ , and  $\text{BaF}_2$ , and comparing the results with experimentally measured data. This comparison is presented in Table V, which shows an agreement of within 5% for the two sets of data.

From the five experimentally measured temperature and pressure derivatives, the derivatives of the SOEM were evaluated by a least-squares fit. The results are shown in Tables VI and VII. From the experimentally measured values of  $[d(\rho_0 W^2)/dP]_{p=0}$ , the three linear combinations of the third-order elastic moduli (TOEM) which are determined by hydrostatic pressure measurements only, viz.,  $C_{111} + 2C_{112}$ ,  $C_{144} + 2C_{166}$ , and  $2C_{112} + C_{123}$ , were evaluated, and are shown in Table VIII.

The errors in the quantities obtained by a least-squares fit are the standard deviations multiplied by 0.675. This was found to be the largest error as compared with all other procedures of error evaluation. It was also found that carrying out the least-squares fits with weights equal to the reciprocals of the standard deviations or with equal weights did not change the results significantly, its only effect being to reduce the computed errors by 10–20%.

The 0°K Debye temperature  $\Theta_0$  may be calculated to a good accuracy for cubic crystals with the aid of

TABLE IV. Pressure dependence of the sound travel time for the five propagation modes.

Mode No.	$\rho v^2$	$(\rho_0 W^2)_{p=0}$	$(dc/dp)_T$
1	$c_{44}$	$1.2250 \pm 0.0041$	$1.297 \pm 0.005$
2	$\frac{1}{2}(c_{12} + c_{12} + 2c_{44})$	$7.2209 \pm 0.0489$	$7.705 \pm 0.054$
3	$\frac{1}{2}(c_{11} - c_{12})$	$0.6393 \pm 0.0037$	$0.8367 \pm 0.0057$
4	$c_{11}$	$6.4669 \pm 0.0555$	$7.067 \pm 0.062$
5	$c_{44}$	$1.3038 \pm 0.0089$	$1.372 \pm 0.009$

TABLE V. Specific heat  $C_V$  for some fluorites. (Units are J/mole deg.)

Material	Calculated value	Measured value
$\text{CaF}_2$	64.19	64.95 <sup>a</sup>
$\text{SrF}_2$	68.75	67.96 <sup>b</sup>
$\text{BaF}_2$	71.28	69.54 <sup>c</sup>
$\text{CdF}_2$	70.14	

<sup>a</sup> H. H. Landholt and R. Bornstein, *Science and Technology* (Springer, Berlin, 1951), Vol. II, Part 4.

<sup>b</sup> Reference 12.

<sup>c</sup> S. S. Todd, *J. Am. Chem. Soc.* **11**, 4115 (1949).

TABLE VI. Temperature derivatives of the SOEM of  $\text{CdF}_2$  at 295°K. (Units are  $10^{-4} \text{ deg}^{-1}$ .)

$\frac{d \ln c_{11}}{dT}$	$\frac{d \ln c_{12}}{dT}$	$\frac{d \ln c_{44}}{dT}$
$-3.712 \pm 0.010$	$-5.075 \pm 0.056$	$-5.329 \pm 0.058$

<sup>15</sup> R. N. Thurston and K. Brugger, *Phys. Rev.* **133**, A1604 (1964).

TABLE VII. Pressure derivatives of the SOEM of  $\text{CdF}_2$  at 295°K.

$\frac{dc_{11}}{dP}$	$\frac{dc_{12}}{dP}$	$\frac{dc_{44}}{dP}$
$7.107 \pm 0.035$	$5.521 \pm 0.066$	$1.353 \pm 0.028$

TABLE VIII. Three combinations of TOEM for  $\text{CdF}_2$ . (Units are  $10^{11} \text{ dyn/cm}^2$ .)

$C_{111} + 2C_{112}$	$C_{144} + 2C_{166}$	$2C_{112} + C_{123}$
$263.0 \pm 3.6$	$73.2 \pm 1.6$	$143.1 \pm 2.6$

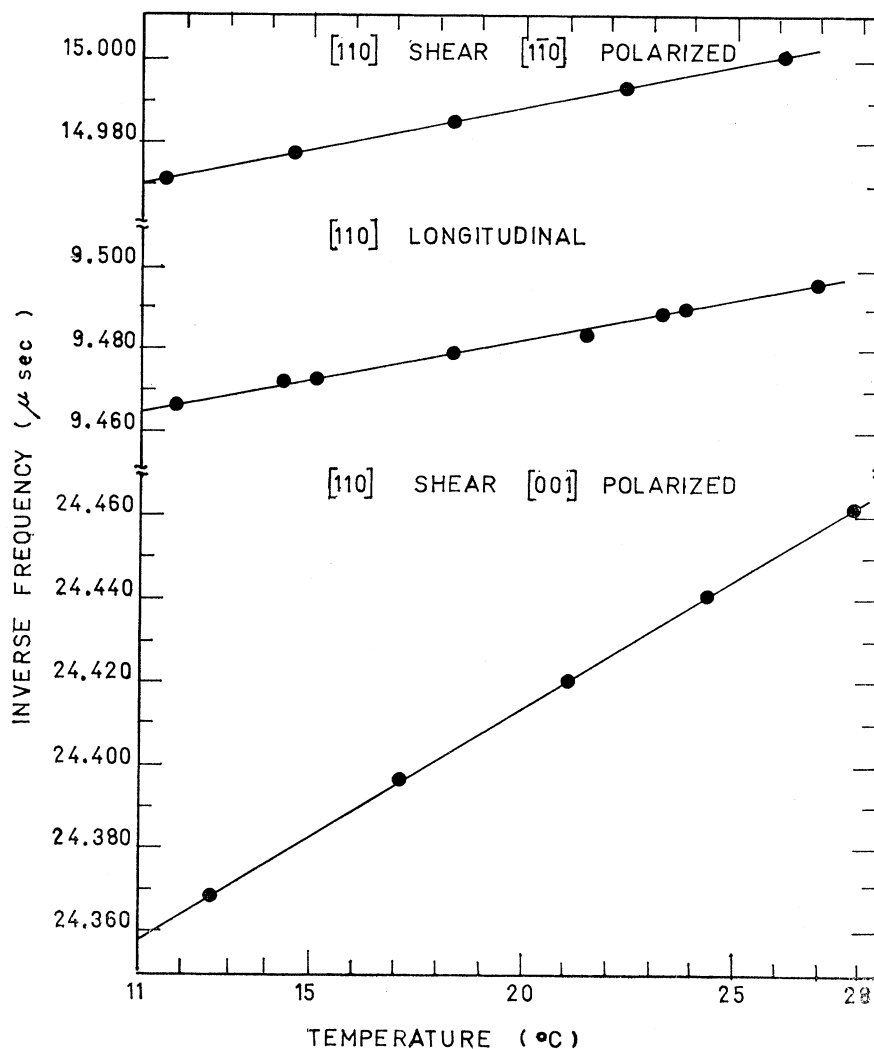


FIG. 2. Reciprocal resonant frequency as a function of temperature for sound propagating in the [110] direction.

De Launy's tables.<sup>16</sup> The SOEM which enter the calculation are, however, 0°K values. In order to determine the latter, the quasiharmonic approximation<sup>17</sup> was used to deduce the 0°K moduli from the room-temperature values and the temperature derivatives. The temperature dependence of the SOEM is given by

$$c_{ij}^S = \tilde{c}_{ij}(1 - D_{ij}\bar{\epsilon}), \quad (5)$$

where  $\tilde{c}_{ij}$  is the 0°K SOEM referred to the static lattice,  $D_{ij}$  is a constant,  $\bar{\epsilon}$  is the average thermal energy given by

$$\bar{\epsilon} = \frac{3}{8}k\tilde{\Theta} + 3k\tilde{\Theta}\left(\frac{T}{\tilde{\Theta}}\right)^4 \int_0^{\tilde{\Theta}/T} \frac{\lambda^3}{\exp(\lambda) - 1} d\lambda. \quad (6)$$

<sup>16</sup> J. De Launy, in *Solid State Physics*, edited by F. Seitz and D. Turnbull (Academic, New York, 1956), Vol. 2.

Here,  $\tilde{\Theta}$  is the harmonic Debye temperature<sup>17</sup> derivable from  $\tilde{c}_{ij}$ . The 0°K SOEM were determined by a self-consistent calculation. Initially, from the room-temperature SOEM the starting value of  $\tilde{\Theta}$  was computed. The latter was utilized in Eqs. (5) and (6) for the determination of the  $\tilde{c}_{ij}$ , the process being repeated three to four times until self-consistency in the values of the  $\tilde{c}_{ij}$  has been achieved.

The validity of the above method was tested using the room-temperature SOEM and their temperature derivatives for CaF<sub>2</sub> and SrF<sub>2</sub> in order to calculate their 0°K SOEM and their Debye temperatures  $\tilde{\Theta}$  and  $\Theta_0$ . The results are shown in Table IX, together with the experimentally measured values. As is evident from the latter table, the agreement between the extrapolated and measured SOEM is within experimental error. The results obtained for CdF<sub>2</sub> are  $\tilde{\Theta} = (337 \pm 3)^\circ\text{K}$ ,  $\Theta_0 = (328 \pm 3)^\circ\text{K}$ .

<sup>17</sup> G. Leibfried and W. Ludwig, in *Solid State Physics*, edited by F. Seitz and D. Turnbull (Academic, New York 1961), Vol. 12

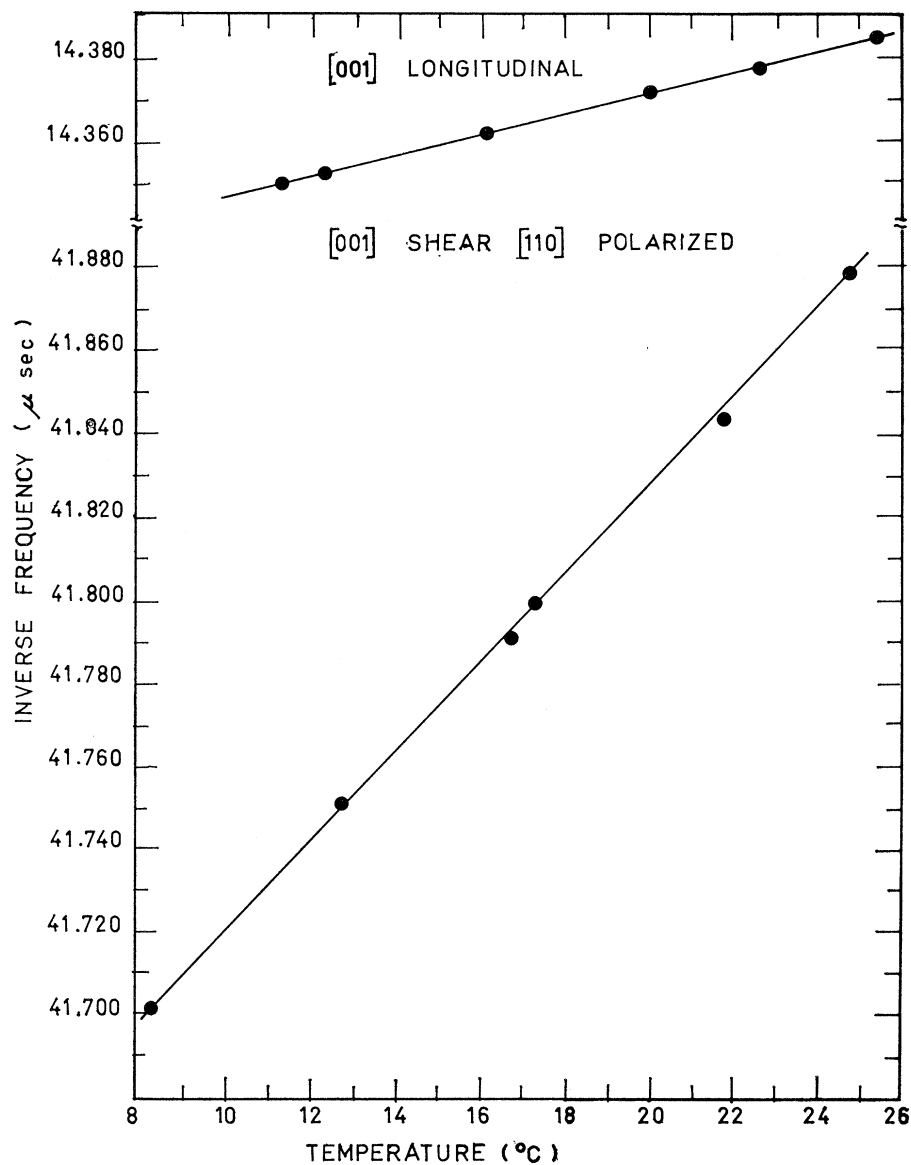


FIG. 3. Reciprocal resonant frequency as a function of temperature for sound propagating in the [001] direction.

TABLE IX. SOEM and Debye temperatures at 0°K for CaF<sub>2</sub>, SrF<sub>2</sub>, and CdF<sub>2</sub>. (Units of SOEM are 10<sup>11</sup> dyn/cm<sup>2</sup>.)

Material	$c_{ij}(T=0^\circ\text{K})$ calc	$\Theta_0$ calc	$c_{ij}(T=0^\circ\text{K})$ expt	$\Theta_0$ expt	$\bar{c}_{ij}$	$\bar{\Theta}$
CaF <sub>2</sub>	$c_{11}$	17.107	17.124 <sup>a</sup>		17.642	
CaF <sub>2</sub>	$c_{12}$	4.708	4.675	519.4 <sup>a</sup>	4.907	528.3
CaF <sub>2</sub>	$c_{44}$	3.601	3.624		3.782	
SrF <sub>2</sub>	$c_{11}$	12.865	12.88 <sup>b</sup>		13.416	
SrF <sub>2</sub>	$c_{12}$	4.678	4.748	380 <sup>b</sup>	4.965	389.2
SrF <sub>2</sub>	$c_{44}$	3.344	3.308		3.556	
CdF <sub>2</sub>	$c_{11}$	19.642	...	...	20.549	
CdF <sub>2</sub>	$c_{12}$	7.357	...	...	7.808	336.9
CdF <sub>2</sub>	$c_{44}$	2.410	...	...	2.565	

<sup>a</sup> Reference 6.

<sup>b</sup> Reference 18.

<sup>18</sup> D. Gerlich, Phys. Rev. **136**, A1336 (1964).

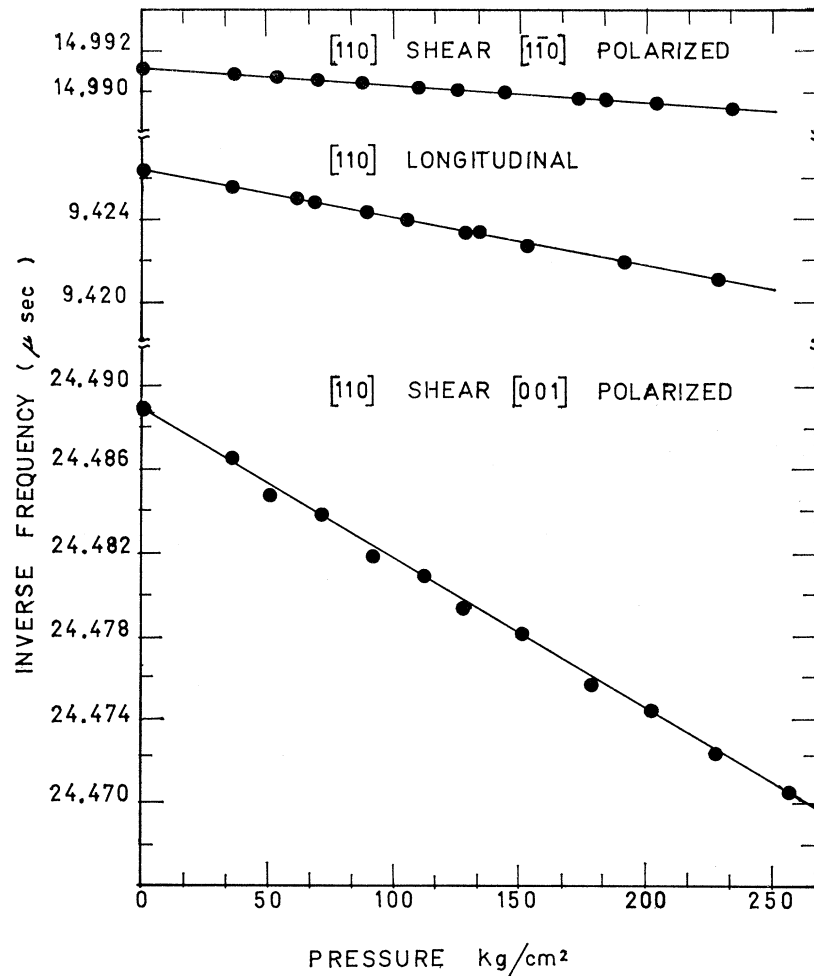


FIG. 4. Reciprocal resonant frequency as a function of pressure for sound propagating in the  $[110]$  direction.

#### IV. DISCUSSION

##### A. Comparison with Theory

The values of  $c_{44}$  and the three linear combinations of the TOEM  $C_{111}+2C_{112}$ ,  $C_{144}+2C_{166}$ , and  $2C_{112}+C_{123}$  were calculated theoretically from a rigid-ion model and a shell model.<sup>1,2,19-21</sup> In both models, a central-force interaction is assumed, consisting of a Coulombic interaction and exchange interactions to next-nearest neighbors. As it has been shown that the exchange interaction with third-nearest neighbors vanishes for the alkaline-earth fluorides,<sup>22</sup> including only second-nearest-neighbor interactions is a justified approximation. The repulsive potential was assumed to be of the form  $A/r^n$ , where  $r$  is the distance between the interacting ions,  $A$  and  $n$  being constants. It was found that varying  $n$  from 6 to 12 changed the three computed

linear combinations of the TOEM and  $c_{44}$  by less than 5%. A value of  $n=10$  was chosen for the computation. Being insensitive to  $n$ , the rigid-ion model has only two parameters  $c_{11}$  and  $c_{12}$ . Their values used in the computation were the harmonic values referred to in the static lattice, viz.,  $\bar{c}_{11}$  and  $\bar{c}_{12}$ .

In the shell-model calculation, two sets of parameters were used for the shell charge  $Y_2$  and the shell-core spring constant  $K_2$  of the cation  $F^-$ : (i) the average values used for the other alkaline-earth fluorides<sup>5,12</sup>  $Y_2 = -1.68$ ,  $K_2 = 6.8 \times 10^5$  dyn/cm; and (ii)  $Y_2$ , as given by Dick,<sup>23</sup> and  $K_2$ , as determined from the free-ion polarizability, i.e.,  $Y_2 = -2.40$ ,  $K_2 = 1.27 \times 10^6$  dyn/cm. The first set of shell-model parameters gave a better agreement with Axe and co-workers'<sup>24</sup> experimental effective charges of  $CdF_2$  than the second one.

In Table X, the results of the theoretical calculation for  $c_{44}$ ,  $C_{111}+2C_{112}$ ,  $C_{144}+2C_{166}$ , and  $2C_{112}+C_{123}$ , together with the experimental data, are shown. As can

<sup>19</sup> J. D. Axe, Phys. Rev. **139**, A1215 (1965).

<sup>20</sup> R. Srinivasan, Phys. Rev. **165**, 1041 (1968).

<sup>21</sup> R. Srinivasan, Phys. Rev. **165**, 1054 (1968).

<sup>22</sup> H. W. Verleur and A. S. Barker, Jr., Phys. Rev. **164**, 1169 (1967).

<sup>23</sup> B. G. Dick, Phys. Rev. **145**, 609 (1966).

<sup>24</sup> J. D. Axe, J. W. Caglianella, and J. E. Scardefuld, Phys. Rev. **139**, A1211 (1965).

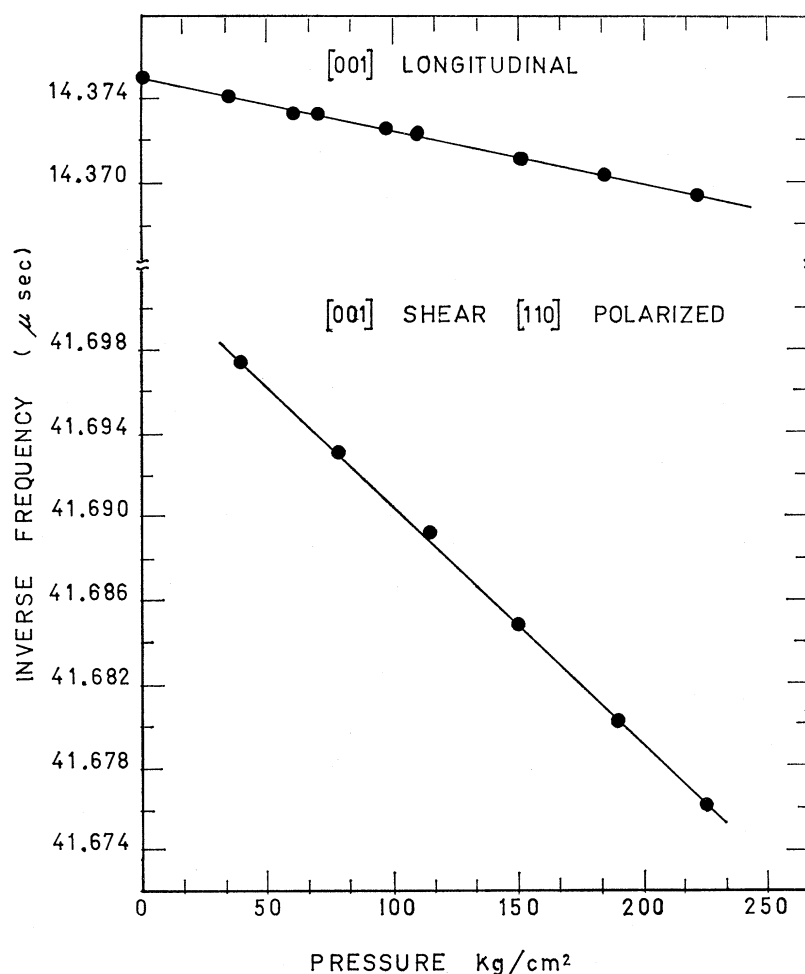


FIG. 5. Reciprocal resonant frequency as a function of pressure for sound propagating in the [001] direction.

be seen, there is good agreement between the measured room-temperature combinations of the TOEM and the 0°K measured ones, while the values of  $c_{44}$  disagree. Although the comparison for the TOEM is made between measured room-temperature data and calculated 0°K values, the TOEM are not expected to be strongly temperature dependent, as is indicated by measurements on  $\text{CaF}_2$  and  $\text{BaF}_2$ .<sup>5,6</sup>

As can be seen from Table X, the model is quite successful in accounting for the measured values of the linear combinations of the TOEM in  $\text{CdF}_2$ . It should also be pointed out that the calculated combinations of the TOEM are very insensitive to the choice of model,

TABLE X. Comparison of the experimental and theoretical elastic constants of  $\text{CdF}_2$ . (Units are  $10^{11}$  dyn/cm<sup>2</sup>.)

	$\tilde{c}_{44}$	$C_{111}+2C_{112}$	$C_{123}+2C_{112}$	$C_{144}+2C_{166}$
Experimental	2.57	263.0	143.1	73.24
Rigid-ion model	6.39	255.4	168.3	89.4
Shell model a	5.48	255.4	168.3	81.7
Shell model b	4.33	255.4	168.3	72.1

as can be seen from the close agreement of the TOEM combinations computed from the rigid-ion and shell models. The reason for this is that the combinations of the TOEM are mainly determined by the core-core interaction. The discrepancy between the calculated and measured values of  $c_{44}$  is noteworthy, especially as in the case of the closely related material  $\text{CaF}_2$ , there is good agreement with experiment, where the calculation is based on the same model as above.<sup>19</sup> It should be pointed out that the electrostatic contribution to  $c_{44}$  is large and negative; thus the calculated value will depend strongly on the short-range interactions, and hence will be quite sensitive to the nature of the assumed model. It is possible that because of the different electronic structures of  $\text{Ca}^{++}$  and  $\text{Cd}^{++}$ , there is a stronger deviation from a two-body central-force interaction in the  $\text{CdF}_2$  than in the  $\text{CaF}_2$  lattice. Since no first-principle calculations of the short-range interaction in the fluorite lattice have been done up to now, this point cannot be further elaborated.

Utilizing the measured pressure derivatives, the explicit temperature dependence of the SOEM may be

TABLE XI. Constitution of the temperature derivatives of the SOEM at 295°K. (Units are  $10^{-4}$  deg $^{-1}$ .)

	$\left(\frac{d \ln c_{ij}}{dT}\right)_P$	$\left(\frac{d \ln c_{ij}}{dT}\right)_V$	$+3\alpha B^T \left(\frac{d \ln c_{ij}}{dP}\right)_T$
$c_{11}$	-3.71	1.12	2.59
$c_{12}$	-5.08	-0.44	5.52
$c_{44}$	-5.33	1.18	4.15

evaluated as follows:

$$\left(\frac{d \ln c_{ij}}{dT}\right)_P = \left(\frac{d \ln c_{ij}}{dT}\right)_V + 3\alpha B^T \left(\frac{d \ln c_{ij}}{dP}\right)_T. \quad (7)$$

Here,  $(d \ln c_{ij}/dT)_P$  is the measured temperature derivative, and  $(d \ln c_{ij}/dT)_V$  is the intrinsic change of the effective SOEM with temperature, which should be zero if the quasiharmonic approximation is strictly applicable. In Table XI, the values of the explicit and implicit temperature derivatives for CdF<sub>2</sub> are presented. As can be seen, the quasiharmonic approximation is a reasonable one for CdF<sub>2</sub> at room temperature.

The Debye temperature may also be evaluated by the Lindemann formula when the melting point of the material is known.<sup>25</sup> Table XII shows the value of the Debye temperature as derived from the elastic data and the Lindemann formula. As can be seen, for CdF<sub>2</sub> the agreement between the two Debye temperatures is of the same order as for the other alkaline-earth fluorides.

### B. Gruneisen Gammas

Utilizing the room temperature and 0°K SOEM together with their pressure derivatives, the mode Gruneisen gammas  $\gamma_i$  ( $i=1, 2, 3$ ), and the low- and high-temperature limits of their thermal average,  $\gamma_L$  and  $\gamma_H$ , may be evaluated.<sup>26</sup> The values thus obtained

TABLE XII. Debye temperature of some fluorides: comparison of Lindeman's formula ( $\Theta_L$ ) and elastic data ( $\Theta_0$ ).

	$\Theta_0$	$\Theta_L$
CdF <sub>2</sub>	328	340
CaF <sub>2</sub>	519	518
SrF <sub>2</sub>	380	360
BaF <sub>2</sub>	282	295

<sup>25</sup> N. F. Mott and H. Jones, *The Theory and Properties of Metals and Alloys* (Dover, New York, 1958).

<sup>26</sup> D. E. Schuele and C. S. Smith, *J. Phys. Chem. Solids* **25**, 801 (1964).

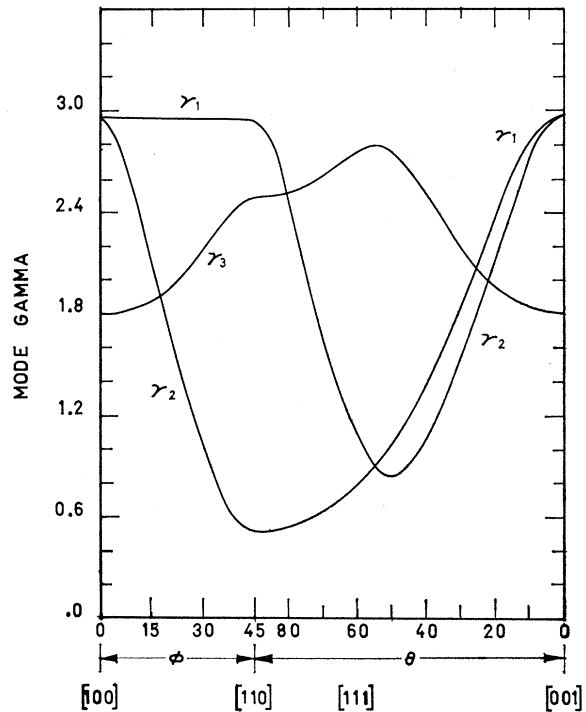


FIG. 6. Mode gammas as a function of crystalline direction.

are  $\gamma_L=2.05$  and  $\gamma_H=1.96$ . The  $\gamma_i$ 's for some directions of high symmetry are shown in Fig. 6, where  $\phi$  denotes the azimuthal angle and  $\theta$  denotes the colatitude; 3 refers to the longitudinal mode, 1 and 2 refer to the slow and fast shear modes, respectively. The value of  $\gamma_H$  deduced from room-temperature thermal expansion is 2.23, which is in fair agreement with  $\gamma_H$  deduced from the elastic data. This is in contrast with the case of the other alkaline-earth fluorides,<sup>4-7,27</sup> where a large discrepancy was found between two values of  $\gamma_H$ . This again may have some bearing on the difference in the electronic structure of Ca<sup>++</sup>, Sr<sup>++</sup>, and Ba<sup>++</sup> on the one hand, and Cd<sup>++</sup> on the other hand.

### ACKNOWLEDGMENT

The authors wish to thank Dr. B. Abeles and the RCA Laboratories, Princeton, N. J. for orienting and cutting the crystal.

<sup>27</sup> D. Gerlich, *Phys. Rev.* **168**, 947 (1968).